Synthesis and Characterization of a Covalent Porphyrin-Cobalt Diimine-Dioxime Dyad for Photoelectrochemical H-2 Evolution

Asterios Charisiadis, Emmanouil Giannoudis, Zoi Pournara, Aimilia Kosma, Vasilis Nikolaou, Georgios Charalambidis, Vincent Artero, Murielle Chavarot-Kerlidou, Athanassios G. Coutsolelos

ARTICLE

Synthesis and Characterization of a Covalent Porphyrin-Cobalt Diimine-Dioxime Dyad for *Photoelectrochemical H_2 Evolution*

Asterios Charisiadis,[a] Emmanouil Giannoudis,[b] Zoi Pournara,[a] Aimilia Kosma,[a] Vasilis Nikolaou,[a] Georgios Charalambidis,*[a] Vincent Artero,[b] Murielle Chavarot-Kerlidou*[b] and Athanassios G. Coutsolelos*[a]

[a] Dr. A. Charisiadis, Z. Pournara, A. Kosma, Dr. V. Nikolaou, Dr. G. Charalambidis and Prof. Dr. A.G. Coutsolelos
Department of Chemistry,
University of Crete,
Laboratory of Bioinorganic Chemistry, Voutes Campus, Heraklion 70013, Crete, Greece.
E-mail: gcharal@uoc.gr, acoutsol@uoc.gr

[b] E. Giannoudis, Dr. V. Artero, Dr. M. Chavarot-Kerlidou
Univ. Grenoble Alpes, CNRS, CEA,
IRIG, Laboratoire de Chimie et Biologie des Métaux,
38000 Grenoble, France.
E-mail: *murielle.chavarot-kerlidou@cea.fr*

Supporting information for this article is given via a link at the end of the document.

Abstract: The utilization of solar energy via photoelectrochemical cells (PEC) towards hydrogen (H_2) production is a promising approach in the field of artificial photosynthesis. In this work, the synthesis and complete characterization of the first covalently linked porphyrin-cobalt diimine-dioxime dyad (ZnP-Co) is reported. The synthetic procedure that was followed is based on simple and high yielding reactions, without using any noble metal. Photophysical investigation of the dyad revealed sufficient electronic communication between the sensitizer and the catalyst in the excited state. Finally, NiO films were sensitized with ZnP-Co and the H_2-evolving photoelectrochemical activity of the resulting photocathode was assessed. The modest performances could be rationalized thanks to photolysis and post-operando characterizations of the system, thus providing some guidelines toward the design of more efficient porphyrin-based assemblies.

Introduction

Inspired by photosynthesis, many researchers have developed artificial photosynthetic systems achieving efficient light-harvesting and solar energy conversion into an electrochemical potential.[1] One step further, the construction of dye-sensitized photoelectrochemical cells (DSPECs) has recently emerged as a highly attractive approach to convert and store solar energy into solar fuels.[2] Water splitting tandem DSPECs are in particular the subject of intense research efforts to produce hydrogen from sunlight and water. Their main limitation lies however in the low efficiency of the photocathodes reported so far, compared to the photoanodes counterpart. Thus, the design of novel H_2-evolving photocathode architectures with high catalytic performance is crucial and a large number of research groups has been motivated and focused their studies towards this target.[2c, 2d, 3]

The first essential component in a dye-sensitized photocathode is the photosensitizer, which should be cost-effective, photo-stable and absorb irradiation to relatively wide part of the sunlight spectrum, possessing mobility and high carrier lifetime as well. Porphyrin derivatives are ideal candidates for that purpose since apart from being analogues to the natural occurring chlorophyll compounds, they also possess all the above features.[4] Additionally, porphyrins can be easily structurally modified through straightforward synthetic procedures,[5] rendering them attractive components for the preparation of covalently linked photosensitizer-catalysts dyads[6] and for the construction of dye-sensitized photocathodes for H_2 production.[7]

Recent literature reports have described the first functional H_2-evolving photocathodes based on a noble metal free covalent dye-catalyst assembly.[8] Herein, we report the synthesis and full characterization of the first example of a covalent porphyrin dye-catalyst assembly based on the same cobalt diimine-dioxime catalyst (**ZnP-Co**) and its integration in an H_2-evolving photocathode (Figure 1).

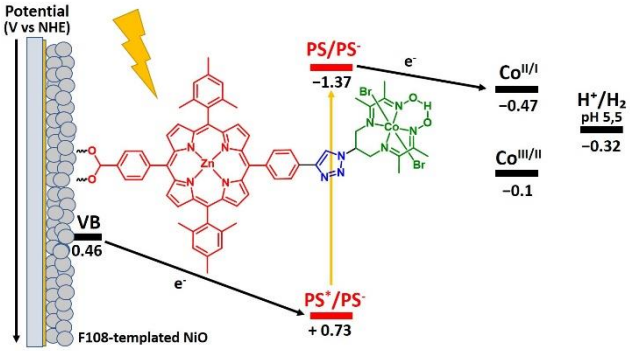

Figure 1. Energy diagram at pH 5.5 and working principle of the NiO photocathode based on **ZnP-Co**. Potentials were converted from Fc to NHE considering $E°(Fc^{+/0})$ = +0.53 V vs NHE. The NiO valence band edge potential at this pH value was estimated from the 0.37 V vs NHE value determined at pH 7.[9]

Based on our previous work, the photosensitizer and catalyst moieties were connected *via* a Cu-catalyzed click reaction.[8a] This

reaction offers facile experimental conditions and in addition, the triazole bridge is reported to provide enhanced electronic communication in porphyrin-based molecular assemblies.[10] For the preparation of the **ZnP-Co** dyad, **ZnP** porphyrin (Figure 2) was used as the main building block. This derivative was also used as reference compound and is functionalized on one side with an alkyne group for the coupling reaction with the catalyst and on the other side with a carboxylic acid group for the anchoring of the dyad onto the NiO surface. We also prepared the methyl-ester analogues of the porphyrin precursor and of the final dyad (Figure 2), in order to achieve enhanced solubility in organic solvents, namely THF, thus enabling their complete characterization in solution.

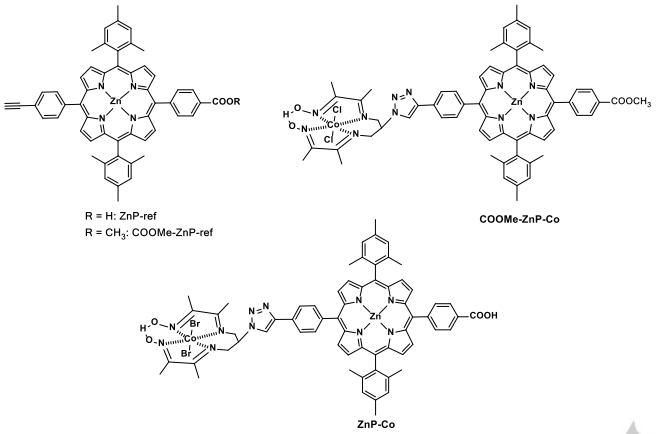

Figure 2. Structures of the two reference compounds (**COOMe-ZnP** and **ZnP**) along with the two dyads (**COOMe-ZnP-Co** and **ZnP-Co**) reported herein**.**

Results and Discussion

The synthetic route that was followed for the preparation of **ZnP-Co** is outlined in Scheme 1 and consisting of six steps.

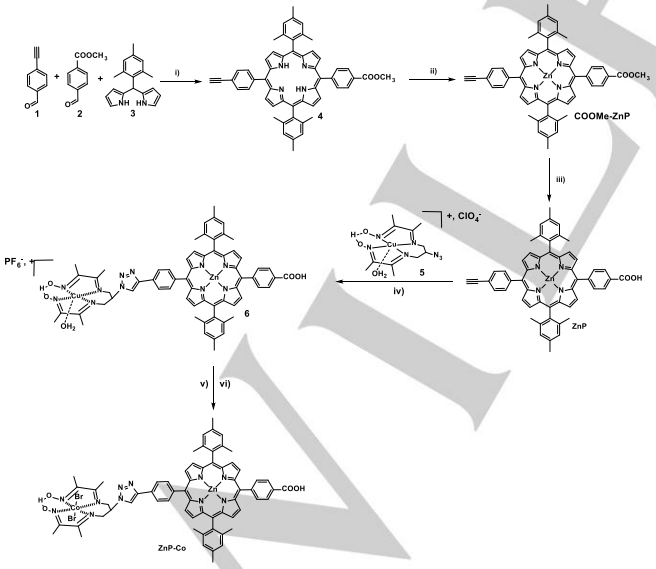

Scheme 1. Synthetic scheme for the **ZnP-Co** dyad. Conditions: i) $CHCl_3$, BF_3OEt_2, 24 h RT, DDQ, 20 h RT; ii) $Zn(CH_3COO)_2{\cdot}2H_2O$, MeOH, CH_2Cl_2; iii) KOH, THF/MeOH/H_2O; iv) $CuSO_4{\cdot}5H_2O$, Sodium ascorbate, CH_2Cl_2/H_2O/MeOH, RT, 24 h; v) $CoCl_2{\cdot}6H_2O$, THF/Acetone, RT, air bubbling, overnight; vi) KBr, THF/Acetone, RT, 5d

In the first step, the acid-catalyzed condensation between dipyrromethane **3**[11] and the aldehydes **1** and **2** took place yielding the free-base porphyrin derivative **4**. Consequently, the macrocycle was metallated with zinc resulting in the formation of **COOMe-ZnP** and then the methylester group was hydrolyzed under basic conditions to provide compound **ZnP**. In the following step, **ZnP** was coupled with the copper diimine-dioxime complex **5**[12] *via* copper(I)-catalyzed azide-alkyne cycloaddition (CuAAC) according to our previously reported protocole**.**[8a, 12] Then, metal exchange was performed through reaction with an excess of $CoCl_2$ in an acetone/THF (1:1) mixture under continuous air bubbling to obtain a stable Co(III) complex. This intermediate was purified through silica-gel flash chromatography and subsequently precipitated in NaBr-saturated aqueous solution to yield the desired dyad (**ZnP-Co**). The procedures that were performed for the preparation of the methyl-ester dyad (**COOMe-ZnP-Co**) are depicted in Scheme S1. A click reaction was also carried out in order to connect **COOMe-ZnP** with complex **5**, followed by a metal exchange reaction. The purity of all intermediates as well as both final dyads (**ZnP-Co** and **COOMe-ZnP-Co**) was confirmed by MALDI-TOF mass spectrometry and NMR spectroscopy (^{1}H and ^{13}C) (Figures S1-S21). Both dyads (**ZnP-Co** and **COOMe-ZnP-Co**) presented in their ^{1}H NMR spectra the characteristic signal for the proton of the oxime bridge in the pseudo-macrocyclic cobalt diimine-dioxime catalyst at 20.07 and 19.28 ppm, respectively; the peak of the newly formed triazole ring is observed at 8.34 and 9.28 ppm, respectively. Moreover, the peak corresponding to the carboxylic acid anchoring group was observed at 13.37 ppm for **ZnP-Co**.

The photophysical characterization of the final dyad as well as the reference porphyrin was performed in their ester analogues *via* absorption and emission spectroscopies. The absorption spectra of **COOMe-ZnP** and **COOMe-ZnP-Co** in THF solutions are presented in Figure S22. The reference derivative illustrates typical zinc porphyrin-based features, i.e. one Soret (425 nm) and two Q bands (557 and 598 nm). These characteristics are also observed in the dyad accompanied by some weak contributions at lower wavelengths, which could be attributed to the cobalt diimine-dioxime catalyst.[8a] Since no significant shift was observed for any of the absorption peaks, but only a slightly decreased absorption coefficient for the Soret band in the dyad, we can safely assume that the two constituent entities interact weakly in the ground state of the dyad.

In an effort to gain some insight into the photoinduced processes that can take place in our dyad, fluorescence experiments were conducted and the emission spectra of **COOMe-ZnP** and **COOMe-ZnP-Co** in THF were compared (Figure 3).

Both the reference compound (**COOMe-ZnP**) and the dyad (**COOMe-ZnP-Co**) exhibited characteristic emission peaks for a zinc porphyrin, located at around 608 and 656 nm. In the case of the dyad, the intensity of both bands is partly quenched upon selective excitation of the porphyrin unit at 555 nm. Two processes might account for this observation: either a thermodynamically allowed electron transfer from the porphyrin excited state to the Co(III) center (ΔG^o = -1.13 eV, see below), or an energy transfer from the first singlet excited state of porphyrin towards the catalyst unit.

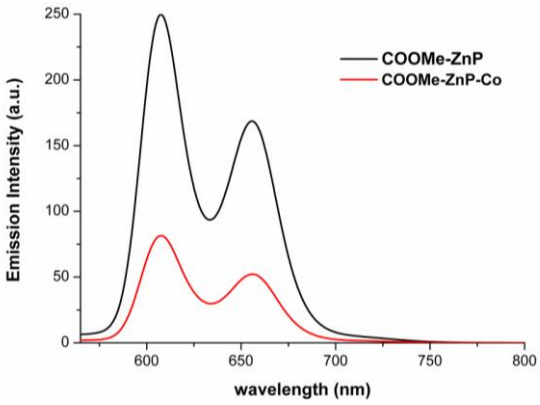

Figure 3. Emission spectra of isoabsorbing solutions of compound **COOMe-ZnP** (black) and **COOMe-ZnP-Co** (red) in THF upon excitation at 555 nm.

The electrochemical properties of **COOMe-ZnP-Co** were determined by cyclic voltammetry (Figure 4) in freshly distilled and deoxygenated tetrahydrofuran with tetrabutylammonium hexafluorophosphate ($TBAPF_6$) as supporting electrolyte. All the electrochemical data are summarized in Table 1.

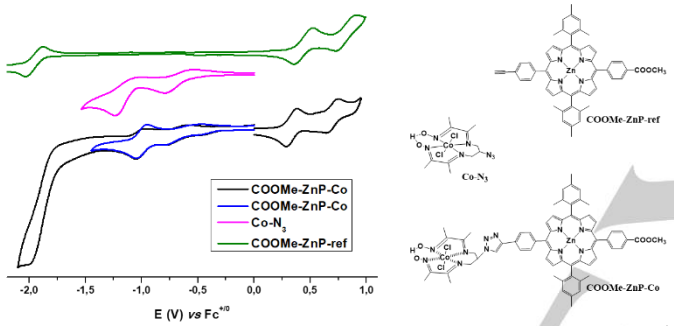

Figure 4. Cyclic voltammograms of **COOMe-ZnP** (top) compared with those of **Co-N₃** (middle) and of the dye precursor **COOMe-ZnP-Co** (bottom).

Three reduction processes and two oxidative waves can be observed in the case of the dyad (Figure 4, bottom). The first two reductive processes at -0.63 V vs Fc and -1.00 V vs Fc were attributed to the $Co^{III/II}$ and $Co^{II/I}$ couples of the catalytic moiety, respectively, by comparison with the cyclic voltammogram of the **Co-N₃** precursor (Figure 4, middle) and with the previously reported dye-catalyst assembly, which displayed similar processes at -0.55 and -1.02 V vs Fc.[8a] In **Co-N₃**, the second process is less reversible and slightly shifted to a more cathodic potential, a behaviour we attribute to some conformational constraints created by the azido substituent. As it has already been reported, this shift of approximately 100 mV of the irreversible reductive wave ($Co^{II/I}$) is assigned to the formation of the triazole ring in the dyad.[13]

Table 1. Summary of the electrochemical redox data of **COOMe-ZnP**, **Co-N₃** and **COOMe-ZnP-Co** in THF. All potentials are reported vs. Fc/Fc^+ which was used as the internal standard.

Name	$E_{(ZnP/ZnP^-)}$ (V)	$E_{Co^{II/I}}$ (V)	$E_{Co^{III/II}}$ (V)	$E_{(ZnP/ZnP^+)}$ (V)	$E_{(ZnP^+/ZnP^{2+})}$ (V)
COOMe-ZnP	-1.96			0.44	0.82
Co-N₃		-1.15	-0.66		
COOMe-ZnP-Co	-1.90	-1.00	-0.63	0.34	0.70

The remaining reductive wave along with both oxidation peaks were assigned to the porphyrin core by comparing the voltammograms of our dyad and the reference dye (Figure 4, top). Both oxidation peaks are slightly cathodically shifted in the dyad compared to the reference dye (approximately 0.1 V), due to the different peripheral substituents of the porphyrin ring, namely triazole ring and ethynyl group, respectively.

Based on the electrochemical data, we estimated a driving force ΔG° of -1.13 eV for the photoinduced electron transfer from ZnP* to the Co(III) center, according to the simplified Rehm–Weller equation:

$\Delta G° = E_{ox}(ZnP/ZnP^+) - E_{00}(ZnP^*) - E_{red}(Co^{III/II})$.

E_{00} stands for the energy of the singlet excited state of the ZnP estimated from the intercept of the absorption and emission spectra as 2.1 eV.

ZnP-Co was then anchored onto homemade F108-templated NiO films. A dyad loading of 6.4 ± 0.9 $nmol.cm^{-2}$ (Table S1) was determined by desorption of the dyad from freshly-sensitized films in a THF solution of 1 M phenylphosphonic acid.[14] Linear sweep voltammograms were recorded in a 2-(*N*-morpholino)ethanesulfonic acid (MES) buffer electrolyte at pH 5.5[8a] under dark, chopped-light and continuous light irradiation conditions (Figure 5), using the **ZnP-Co**-sensitized photocathode as working electrode in a three-electrode setup. The experimental conditions that were followed herein are based on our previous light-driven H_2 evolution studies with covalent dye–catalyst assemblies.[8a] Cathodic photocurrents are clearly generated under visible light irradiation (Figure 5) from +0.94 V vs RHE, reaching up to 11 $\mu A.cm^{-2}$ (dark current subtracted). To assess whether these photocurrents are correlated with photoelectrocatalytic hydrogen production, two hours chronoamperometric measurements coupled to hydrogen detection were carried out (Figure S23) at -0.4 V vs Ag/AgCl for direct comparison with our previously-reported photocathodes based on the same cobalt diimine dioxime catalyst.[8]

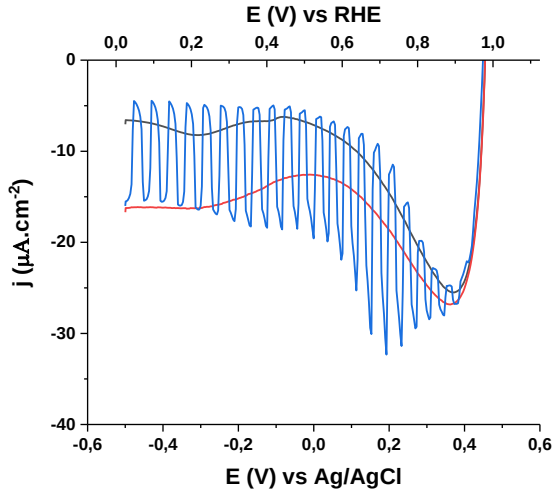

Figure 5. Linear sweep voltammograms of **ZnP-Co**–sensitized NiO electrodes, recorded in a pH 5.5 MES 0.1 M/NaCl 0.1 M buffer under dark conditions (black line), continuous visible light irradiation (red line) or chopped light irradiation (blue line).

At the end of the experiments, the amount of hydrogen produced was measured in the headspace and in the electrolyte solution,[8b] reaching 8 ± 1% Faradaic Efficiency (F.E.) and 7 ± 1 nmol.cm^{-2}. Similarly low F.E., ranging from 6 to 13 %, were also obtained for the previously-reported dye-sensitized H_2-evolving photocathodes based on the same cobalt diimine-dioxime catalyst;[8, 15] the reason behind this is still not clearly understood although it might be related to the reduction of some O_2 trapped within the mesoporous NiO structure or to some degradation pathways. By comparison, control experiments performed with **ZnP**-sensitized NiO films under identical conditions produced only 3 nmol.cm^{-2} (Table S1).

Post-operando characterization of the dyad was performed after desorption from the film in a 1 M phenylphosphonic acid solution in THF. The UV-vis spectrum of the solution displays an overall lower intensity of the porphyrin characteristic signals by comparison with the spectrum recorded after desorption of the freshly-sensitized film (Figure 6); this indicates that some desorption of **ZnP-Co** from the NiO surface (estimated to ≈ 40 %) occurred during the course of the two-hours photo-electrochemical experiment. In addition, a clear increase in the number of Q bands is observed. This can be attributed either to the demetallation of the porphyrin core,[16] or to the formation of chlorin species due to the reduction/hydrogenation of the porphyrin ring.[17] As demetallation of porphyrins is reported to take place under acidic conditions,[16] the photoelectrocatalytic activity of the films was also assessed at pH 7. Although the **ZnP-Co**-sensitized film displays improved stability at this less acidic pH (desorption ≈ 25 %, see Figure S24), the activity was not enhanced and the same amount of hydrogen was produced (Table S1).

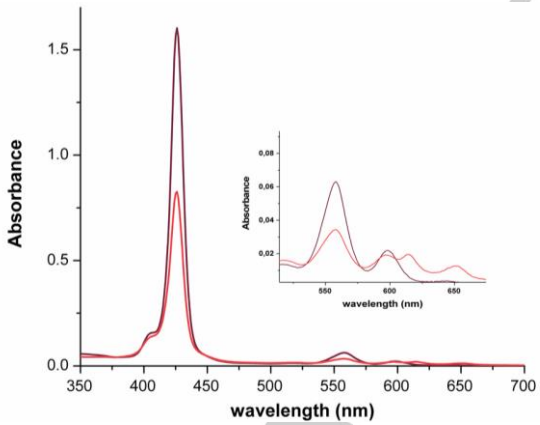

Figure 6. UV-vis absorption spectra of desorption solutions (1 M phenylphosphonic acid in THF) of a fresh **ZnP-Co**-sensitized NiO film (black line) and the same sample (second half of the same sensitized film; red line) after a two-hours chronoamperometric measurement under continuous light irradiation at an applied potential of –0.4 V vs Ag/AgCl in MES buffer pH 5.5.

The overall performances of this novel dyad are slightly lower than the ones previously reported for a NiO-based photocathode based on the same cobalt diimine-dioxime complex covalently coupled with a push-pull organic dye.[8a] In order to ascertain whether electrons are transferred to the catalytic center within the dyad, a UV-vis-monitored photolysis experiment was performed in a THF solution of **COOMe-ZnP-Co**, using triethanolamine (TEOA) as sacrificial electron donor (Figure S25). Unfortunately, in all conducted experiments we could neither observe the accumulation of the Co(II) state nor the one of the Co(I) state of the catalyst, which is in sharp contrast with our previous dyads.[8a, 18] The newly-formed peak at approximately 620 nm is ascribed to the reduced form of the porphyrin macrocycle, generated upon reductive quenching of the excited state of the latter by TEOA.[19] Accumulation of the reduced porphyrin during the course of the photolysis experiment thus clearly indicates that electron transfer to the catalyst is not efficient although this process is thermodynamically favored. Compared to our dye-catalyst assemblies based on a push-pull organic dye, a lack of directionality for the electron transfer from the porphyrin core to the catalytic center can be invoked to support these observations. Indeed, the electron-withdrawing ability of the carboxylate anchoring group most probably stabilizes the electron on the opposite side of the cobalt complex, preventing the formation of the catalytically active species and accounting for the low photoelectrocatalytic activity of the **ZnP-Co** sensitized photocathode.

Conclusion

To sum up, a new noble metal-free dyad was synthesized by employing click chemistry reaction in order to covalently connect a zinc-porphyrin sensitizer with a H_2-evolving cobalt diimine dioxime catalyst. We have also prepared the methyl-ester analogue of the dyad to determine the electrochemical features of our novel system. In the cyclic voltammogram of **COOMe-ZnP-Co** we observed five redox potentials, which were assigned to either the chromophore or catalytic unit by comparison with the corresponding voltammograms of both precursors (**COOMe-ZnP** and **Co-N$_3$**, respectively). Additionally, we performed photolysis experiments in the **COOMe-ZnP-Co** dyad in order to further evaluate the electronic communication between the zinc porphyrin and the catalyst. However, we did not observe the formation of the desired Co(I) species, hence suggesting that an electron shift from the porphyrin to the cobalt diimine-dioxime moiety does not take place easily. Finally, dye-sensitized photocathodes were constructed incorporating both the **ZnP-Co** dyad and the **ZnP** dye and their photoelectrochemical activity was assessed under pertinent conditions.

This is the first attempt to prepare a noble metal free covalently connected porphyrin-cobalt dyad targeting its utilization in PEC for H_2 production. All the results in this study highlight the importance of developing novel photosensitizer-catalyst entities for photo-electrocatalytic reduction reactions of interest in the context of a solar-driven chemistry. Several modifications should be explored in future research works examining crucial factors that impact the catalytic efficiency as well as the stability of the dyad onto the photocathode. Namely, the insertion of a non-conjugated methylene spacer between the anchoring group and the porphyrin ring will decrease the electronic coupling with NiO, and in turn slow down unwanted recombination processes.[20] In addition, introducing electron donating moieties on the periphery of the porphyrin macrocycle could possibly assist the charge transfer process from the sensitizer to the catalyst. Finally, a thorough investigation regarding different anchoring groups of the photosensitizer, such as phosphonic acid, hydroxamic acid or alkoxysilane, is required to increase the stability of the dyad onto the photocathode and enhance the catalytic activity. Alternatively, atomic layer deposition (ALD) deposition of a thin layer of alumina

would prevent the dyad release in solution. Optimizing all the above mentioned parameters will allow to develop better performing photocathodes for H_2 evolution based on noble metal free porphyrin light harvesting units.

Experimental Section

Materials and techniques. Reagents and solvents were purchased as reagent grade from usual commercial sources and were used without further purification, unless otherwise stated. NMR spectra were recorded on a Bruker AVANCE III-500 MHz spectrometer using solutions in deuterated solvents and the solvent peak was chosen as the internal standard. A Bruker UltrafleXtreme matrix assisted laser desorption ionization time-of-flight (MALDI-TOF) spectrometer was used to record the mass spectra and trans-2-[3-(4-tert-butylphenyl)-2-methyl-2-propenylidene] malononitrile (DCTB) was selected as matrix.

Photophysical Measurements. Absorption spectra were obtained using a Shimadzu UV-1700 spectrophotometer and steady-state emission spectra were recorded on a JASCO FP-6500 fluorescence spectrophotometer.

Electrochemistry. Cyclic voltammetry experiments were carried out at room temperature using an AutoLab PGSTAT20 potentiostat. All measurements were carried out in freshly distilled and deoxygenated THF in the presence of 0.1 M of tetrabutylammonium hexafluorophosphate ($TBAPF_6$) as the supporting electrolyte, at a scan rate of 100 mV s^{-1}. A three-electrode cell setup was used with a glassy carbon working electrode, an Ag/AgCl reference electrode, and a platinum wire as a counter electrode. In all measurements the potential of the reference electrode was calibrated vs the electrolyte ferrocenium-ferrocene ($Fc^{+/0}$) couple, by adding in the supporting electrolyte of each experiment, ferrocene as an internal reference.

Photoelectrochemical measurements. For a typical photoelectrocatalytic experiment, irradiation was carried out with a 300W ozone-free Xe lamp operated at 280 W equipped with a water-filled filter for elimination of IR irradiation (Spectra-Physics 6123NS) and a UV cut-off filter (Spectra-Physics 59472, λ > 400 nm). The power density was calibrated to 65 mW·cm^{-2} (≈1 sun) using a 60% optical density filter using a Newport PM1918-R power-meter. The experiments were performed in a three-electrode cell, using the NiO-sensitized film as working electrode (3.3 to 3.3 cm^2, accurately measured for each experiment), Ag/AgCl as the reference electrode and a Pt wire as the auxiliary electrode. The supporting electrolyte was 0.1 M 2-(N-morpholino)ethanesulfonic acid (MES) / 0.1 M NaCl buffer at pH 5.5 or Britton-Robinson buffer at pH 7. The volume of supporting electrolyte (around 5 mL) and the headspace volume (around 2 mL) were accurately measured for each single experiment. The different compartments of the cell and the electrolyte were degassed for 30 minutes before the PEC experiments. The amounts of evolved hydrogen were determined after two hours of chronoamperometry run by sampling 50 µL of the headspace in Perkin Elmer Clarus 580 gas chromatograph equipped with a molecular sieve 5 Å column (30m – 0.53 mm) and by micro-clark electrode in the electrolyte solution.[8b]

Linear sweep voltammograms (LSV). Prior to the long-term chronoamperometric experiments, linear sweep voltammograms were recorded for each sensitized NiO film under dark conditions (lamp off), then continuous irradiation (lamp on), then chopped light irradiation (lamp on-off), screening from + 0.5 V to - 0.5 V vs Ag/AgCl with a scan rate of 10 mV.s^{-1}.

Film sensitization. F108-templated NiO films were prepared according to our previously reported procedure.[8a] Sensitization was achieved by soaking them for 24h in 0.1 mM **ZnP-Co** or **ZnP** THF solutions. Finally, the films were soaked in pure THF to remove physiosorbed compounds from the surface and dried under air flow.

Determination of the surface concentration in ZnP-Co (or ZnP). Every film was cut in half after sensitization. One half was used to determine the surface concentration and the other half was used for the assessment of the PEC activity. The freshly grafted half of the film was dipped for 4 hours in 5 mL of 1 M phenylphosphonic acid THF solution in order to desorb the dyad from the surface, according to a previously reported procedure.[14] The UV-Visible absorption spectrum of the desorption solution was then recorded to determine the amount of grafted complex from the molar extinction coefficient at the Soret band. Knowing the surface concentrations in **ZnP-Co** allowed us to calculate turn-over numbers (TON) based on the amount of catalyst present at the surface of the film. A similar desorption procedure was applied to the other half of the film after the PEC measurements for post-operando analysis.

Synthesis of **4**. In a two-neck round bottom flask, dipyrromethane **3** (500 mg, 1.9 mmol), 4-ethynylbenzaldehyde **1** (124 mg, 0.95 mmol) and methyl-4-formylbenzale (**2**) (156 mg, 0.95 mmol) were dissolved in 250 mL of $CHCl_3$. The reaction mixture was subsequently bubbled under N_2 for 15 min followed by addition of BF_3OEt_2 (75 µL) and stirring for 24 h. Then, 300 mg of DDQ were added and the mixture was additionally left stirring for 20 h. The resulting product was filtered through a silica pad and afterwards purified via column chromatography (silica gel, Hexane/CH_2Cl_2 in 7:3 ratio) providing 150 mg of porphyrin **4** (yield = 20%). ^{1}H NMR (500 MHz, $CDCl_3$): δ = 8.79 (d, J = 4.7 Hz, 2H), 8.75 (d, J = 4.7 Hz, 2H), 8.72 (d, J = 4.7 Hz, 4H), 8.43 (d, J = 8.4 Hz, 2H), 8.32 (d, J = 8.4 Hz, 2H), 8.20 (d, J = 8.3 Hz, 2H), 7.89 (d, J = 8.3 Hz, 2H), 7.29 (s, 4H), 4.11 (s, 3H), 3.32 (s, 1H), 2.63 (s, 6H), 1.85 (s, 12H), -2.64 (s, 2H) ppm. ^{13}C NMR (75 MHz, $CDCl_3$): δ = 167.5, 147.0, 142.7, 140.5, 139.5, 138.9, 138.3, 138.2, 138.0, 134.7, 134.5, 130.7, 129.3, 128.6, 128.0, 127.9, 121.7, 118.8, 118.7, 118.3, 118.2, 83.8, 78.4, 52.6, 21.8, 21.6 ppm. MS (MALDI-TOF): calculated for $C_{54}H_{44}N_4O_2$ $[M]^+$ 780.3464; found 780.3452.

Synthesis of **COOMe-ZnP**. To a 40 mL CH_2Cl_2 solution of **4** (78 mg, 0.10 mmol), a MeOH (6 mL) solution containing $Zn(CH_3COO)_2{\cdot}2H_2O$ (215 mg, 1 mmol) was added and the reaction mixture was stirred at room temperature (RT) overnight. The solvents were evaporated under reduced pressure and the resulting residue was purified by column chromatography (silica gel, using Hexane/CH_2Cl_2 as eluent in a 7:3 ratio). The formed metallated porphyrin derivative **COOMe-ZnP** was obtained in quantitative yield, namely 98% (80 mg). ^{1}H NMR (500 MHz, $CDCl_3$): δ = 8.87 (d, J = 4.6 Hz, 2H), 8.83 (d, J = 4.6 Hz, 2H), 8.80 (m, 4H), 8.40 (d, J = 8.3 Hz, 2H), 8.32 (d, J = 8.3 Hz, 2H), 8.21 (d, J = 8.2 Hz, 2H), 7.88 (d, J = 8.2 Hz, 2H), 7.29 (s, 4H), 4.08 (s, 3H), 3.31 (s, 1H), 2.64 (s, 6H), 1.84 (s, 12H) ppm. ^{13}C NMR (75 MHz, $CDCl_3$): δ = 167.6, 150.2, 150.1, 149.8, 149.6, 147.9, 143.6, 139.3, 139.0, 138.0, 137.7, 134.6, 134.5, 132.3, 132.1, 131.8, 131.6, 131.2, 131.1, 130.5, 129.9, 129.3, 127.8, 121.4, 119.7, 119.5,

119.2, 119.0, 83.9, 78.3, 52.5, 21.8, 21.6 ppm. MS (MALDI-TOF): calculated for $C_{54}H_{43}N_4O_2Zn$ $[M+H]^+$ 843.2677; found 843.2689.

Synthesis of **ZnP**. To a THF (17 mL) and MeOH (8 mL) mixed solution of **COOMe-ZnP** (65 mg, 0.08 mmol), an aqueous solution (9 mL) of KOH (430 mg, 7.70 mmol) was added. The reaction mixture was stirred at room temperature for two days and then the solvents were evaporated under vacuum and distilled H_2O (10 mL) was added to the resulting residue. The mixture was acidified using HCl(aq) 1 M resulting in the precipitation of derivative as a purple solid which after being filtered, washed with distilled water and dried, was collected (62 mg, 97%). ^{1}H NMR (500 MHz, $CDCl_3$): δ = 8.80 (m, 8H), 8.51 (db, J = 5.9 Hz, 2H), 8.38 (d, J = 7.4 Hz, 2H), 8.21 (d, J = 7.5 Hz, 2H), 7.89 (d, J = 6.9 Hz, 2H), 7.29 (s, 4H), 3.31 (s, 1H), 2.64 (s, 6H), 1.84 (s, 12H) ppm. ^{13}C NMR (125 MHz, $CDCl_3$): δ = 171.2, 150.3, 150.2, 149.9, 149.6, 148.8, 143.3, 139.3, 139.0, 137.7, 134.7, 134.5, 132.4, 132.1, 131.3, 130.5, 130.3, 128.5, 127.9, 121.4, 119.8, 119.7, 118.9, 83.9, 78.3, 52.5, 21.8, 21.6 ppm. MS (MALDI-TOF): calculated for $C_{53}H_{40}N_4O_2Zn$ $[M]^+$ 828.2443; found 828.2451.

Synthesis of **6**: **ZnP** (62 mg, 0.07 mmol) and copper diamine-dioxime complex **5** (26 mg, 0.07 mmol) were solubilized in CH_2Cl_2 (5 mL) under Ar. A solution of $CuSO_4{\cdot}5H_2O$ (12 mg, 0.05 mmol) and sodium ascorbate (28 mg, 0.14 mmol) in Ar-purged water (2 mL) was added. Then, Ar-degassed CH_3OH (5 mL) was added to the biphasic mixture until a single phase was obtained. The reaction mixture was stirred at RT under Ar. After 24 h the solution was concentrated under vacuum yielding a precipitate, which was filtered and washed with water. The solid was purified by flash chromatography on silica gel using as eluent a mixture CH_3CN/aqueous KNO_3 solution at 10% of the saturating concentration. The pure product was obtained after evaporation of CH_3CN in the combined fractions and precipitation by addition of a KPF_6-saturated aqueous solution. The precipitate was filtered, washed with water and dried under vacuum to give dyad **6** as red-brown brick solid (65 mg, 74% yield), which was directly used for the next step.

Synthesis of **ZnP-Co**. Dyad **6** (65 mg, 0.05 mmol) and $CoCl_2{\cdot}6H_2O$ (132 mg, 0.55 mmol) were solubilized in an acetone/THF (1:1) mixture (30 mL) and stirred overnight under air bubbling. After the reaction reached completion, the solution was evaporated under vacuum and the solid was purified by flash chromatography on silica gel using as eluent a mixture of CH_3CN and aqueous KNO_3 solution at 10% of the saturating concentration, then a solution of acetone saturated in NaI to completely desorb the product from the silica gel. The desired fractions were combined and the organic solvents were evaporated under vacuum, yielding a precipitate that was filtered and washed with water. The solid was re-solubilized in an acetone/THF (1:1) mixture. To this solution a NaBr-saturated aqueous solution (a third of the final volume) is subsequently added. The mixture was stirred at RT for five days to allow the organic solvents to slowly evaporate, giving a precipitate. This precipitate was filtered, washed with water and dried under vacuum to obtain the expected **ZnP-Co** dyad as a purple solid (18 mg, 33% yield). ^{1}H NMR (500 MHz, DMF-d_7): δ = 20.07 (s, 1H), 13.37 (sb, 1H), 8.94 (m, 2H), 8.84 (d, J = 4.5 Hz, 2H), 8.69 (m, 4H), 8.47 (d, J = 7.5 Hz, 2H), 8.39 (d, J = 7.7 Hz, 2H), 8.34 (sb, 1H), 8.16 (d, J = 8.0 Hz, 2H), 8.02 (m, 2H), 7.38 (s, 4H), 6.14 (m, 1H), 4.61 (db, J = 14.3 Hz, 2H), 4.48 (m, 2H), 2.63 (s, 6H), 2.49 (s, 6H), 2.28 (s, 6H), 1.86 (m, 12H) ppm. ^{13}C NMR (125 MHz, DMF-d_7): δ = 174.2, 168.0, 156.4, 150.2, 149.9, 149.7, 149.6, 148.1, 139.8, 139.0, 137.6, 134.9, 134.3, 132.5, 132.0, 130.5, 130.2, 127.9, 126.1, 125.5, 123.7, 118.7, 58.9, 53.5, 21.3, 20.9, 17.2, 12.6 ppm. MS (MALDI-TOF): calculated for $C_{64}H_{56}Br_2CoN_{11}O_4Zn$ $[M]^+$ 1323.1507; found 1323.1522.

Acknowledgements

This research was funded by the General Secretariat for Research and Technology (GSRT) and Hellenic Foundation for Research and Innovation (HFRI; project code: 508). This research has also been co-financed by the European Union and Greek national funds through the Operational Program Competitiveness, Entrepreneurship, and Innovation, under the call RESEARCH−CREATE−INNOVATE (project code: T1EDK-01504). In addition, this research has been co-financed by the European Union and Greek national funds through the Regional Operational Program "Crete 2014-2020," project code OPS:5029187. Moreover, the European Commission's Seventh Framework Program (FP7/2007-2013) under grant agreement no. 229927 (FP7-REGPOT-2008-1, Project BIO-SOLENUTI), the Special Research Account of the University of Crete and the French National Research Agency in the framework of the "Investissements d'avenir" program (ANR-15-IDEX-02, Labex ARCANE and CBH-EURGS, ANR-17-EURE-0003) are gratefully acknowledged for the financial support of this research.

Keywords: Porphyrin-cobalt diamine dioxime dyad • photosensitizer-catalyst dyad • "click" chemistry • H_2 evolution • photoelectrochemical cells (PEC)

References

[1] a) A. Agosti, M. Natali, L. Amirav, G. Bergamini, *ChemSusChem* **2020**, *13*, 4894-4899; b) J. H. Kim, D. Hansora, P. Sharma, J.-W. Jang, J. S. Lee, *Chem. Soc. Rev.* **2019**, *48*, 1908-1971; c) Y.-J. Yuan, Z.-T. Yu, D.-Q. Chen, Z.-G. Zou, *Chem. Soc. Rev.* **2017**, *46*, 603-631; d) J. Bonin, A. Maurin, M. Robert, *Coord. Chem. Rev.* **2017**, *334*, 184-198; e) S. Berardi, S. Drouet, L. Francàs, C. Gimbert-Suriñach, M. Guttentag, C. Richmond, T. Stoll, A. Llobet, *Chem. Soc. Rev.* **2014**, *43*, 7501-7519.

[2] a) F. Li, K. Fan, B. Xu, E. Gabrielsson, Q. Daniel, L. Li, L. Sun, *J. Am. Chem. Soc.* **2015**, *137*, 9153-9159; b) J. Willkomm, K. L. Orchard, A. Reynal, E. Pastor, J. R. Durrant, E. Reisner, *Chem. Soc. Rev.* **2016**, *45*, 9-23; c) E. A. Gibson, *Chem. Soc. Rev.* **2017**, *46*, 6194-6209; d) V. Nikolaou, A. Charisiadis, G. Charalambidis, A. G. Coutsolelos, F. Odobel, *J. Mater. Chem. A* **2017**, *5*, 21077-21113; e) M. K. Brennaman, R. J. Dillon, L. Alibabaei, M. K. Gish, C. J. Dares, D. L. Ashford, R. L. House, G. J. Meyer, J. M. Papanikolas, T. J. Meyer, *J. Am. Chem. Soc.* **2016**, *138*, 13085-13102; f) F. Li, H. Yang, W. Li, L. Sun, *Joule* **2018**, *2*, 36-60.

[3] a) Z. Yu, F. Li, L. Sun, *Energy Environ. Sci.* **2015**, *8*, 760-775; b) N. Queyriaux, N. Kaeffer, A. Morozan, M. Chavarot-Kerlidou, V. Artero, *J. Photochem. Photobiol. C* **2015**, *25*, 90-105.

[4] a) P. v. R. Schleyer, *Chem. Rev.* **2001**, *101*, 1115-1118; b) K. M. Kadish, K. M. Smith, R. Guilard, in *The Porphyrin Handbook* (Eds.: K. M. Kadish, K. M. Smith, R. Guilard), Academic Press, Amsterdam, **2003**, p. vii.

[5] S. Hiroto, Y. Miyake, H. Shinokubo, *Chem. Rev.* **2017**, *117*, 2910-3043.

[6] a) Y. Kuramochi, Y. Fujisawa, A. Satake, *J. Am. Chem. Soc.* **2020**, *142*, 705-709; b) K. Ladomenou, M. Natali, E. Iengo, G. Charalampidis, F. Scandola, A. G. Coutsolelos, *Coord. Chem. Rev.* **2015**, *304-305*, 38-54.

[7] a) B. Shan, A. Nayak, R. N. Sampaio, M. S. Eberhart, L. Troian-Gautier, M. K. Brennaman, G. J. Meyer, T. J. Meyer, *Energy Environ. Sci.* **2018**, *11*, 447-455; b) B. Shan, B. D. Sherman, C. M. Klug, A. Nayak, S. L. Marquard, Q. Liu, R. M. Bullock, T. J. Meyer, *J. Phys. Chem. Lett.* **2017**, *8*, 4374-4379.

[8] a) N. Kaeffer, J. Massin, C. Lebrun, O. Renault, M. Chavarot-Kerlidou, V. Artero, *J. Am. Chem. Soc.* **2016**, *138*, 12308-12311; b) C. D. Windle, J. Massin, M. Chavarot-Kerlidou, V. Artero, *Dalton Trans.* **2018**, *47*, 10509-10516.

[9] G. Natu, P. Hasin, Z. Huang, Z. Ji, M. He, Y. Wu, *ACS Appl. Mater. Interfaces* **2012**, *4*, 5922-5929.

[10] K. Ladomenou, V. Nikolaou, G. Charalambidis, A. G. Coutsolelos, *Coord. Chem. Rev.* **2016**, *306*, 1-42.

[11] J. K. Laha, S. Dhanalekshmi, M. Taniguchi, A. Ambroise, J. S. Lindsey, *Org. Process Res. Dev.* **2003**, *7*, 799-812.

[12] N. Queyriaux, E. S. Andreiadis, S. Torelli, J. Pecaut, B. S. Veldkamp, E. A. Margulies, M. R. Wasielewski, M. Chavarot-Kerlidou, V. Artero, *Faraday Discuss.* **2017**, *198*, 251-261.

[13] P. B. Pati, L. Zhang, B. Philippe, R. Fernández-Terán, S. Ahmadi, L. Tian, H. Rensmo, L. Hammarström, H. Tian, *ChemSusChem* **2017**, *10*, 2480-2495.

[14] a) D. Ameline, S. Diring, Y. Farre, Y. Pellegrin, G. Naponiello, E. Blart, B. Charrier, D. Dini, D. Jacquemin, F. Odobel, *RSC Adv.* **2015**, *5*, 85530-85539; b) S. Lyu, J. Massin, M. Pavone, A. B. Muñoz-García, C. Labrugère, T. Toupance, M. Chavarot-Kerlidou, V. Artero, C. Olivier, *ACS App. Energy Mater.* **2019**, *2*, 4971-4980.

[15] N. Kaeffer, C. D. Windle, R. Brisse, C. Gablin, D. Leonard, B. Jousselme, M. Chavarot-Kerlidou, V. Artero, *Chem. Sci.* **2018**, *9*, 6721-6738.

[16] Y. Saga, S. Hojo, Y. Hirai, *Bioorg. Med. Chem.* **2010**, *18*, 5697-5700.

[17] C. D. Windle, M. V. Câmpian, A.-K. Duhme-Klair, E. A. Gibson, R. N. Perutz, J. Schneider, *Chem. Commun.* **2012**, *48*, 8189-8191.

[18] N. Kaeffer, M. Chavarot-Kerlidou, V. Artero, *Acc. Chem. Res.* **2015**, *48*, 1286-1295.

[19] a) C.-Y. Huang, Y. O. Su, *Dalton Trans.* **2010**, *39*, 8306-8312; b) H. Tamiaki, A. R. Holzwarth, K. Schaffner, *J. Photochem. Photobiol. B* **1992**, *15*, 355-360; c) V. Pale, T. Nikkonen, J. Vapaavuori, M. Kostiainen, J. Kavakka, J. Selin, I. Tittonen, J. Helaja, *J. Mater. Chem. C* **2013**, *1*, 2166-2173.

[20] N. Queyriaux, R. A. Wahyuono, J. Fize, C. Gablin, M. Wächtler, E. Martinez, D. Léonard, B. Dietzek, V. Artero, M. Chavarot-Kerlidou, *J. Phys. Chem. C* **2017**, *121*, 5891-5904.

Entry for the Table of Contents

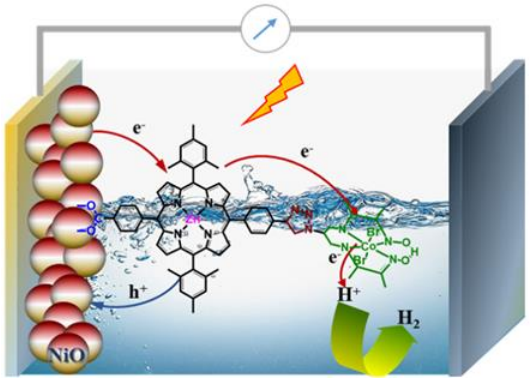

Herein, we report the synthesis of the first covalently linked porphyrin-cobalt diimine-dioxime dyad (ZnP-Co). Using various spectroscopic techniques for the characterization of the dyad, we were observed that a photoinduced electron transfer from ZnP* to the Co(III) center of the catalyst takes place in our system. Based on these findings, the photosensitizer-catalyst dyad was later tested in photoelectrochemical cells towards H_2 evolution.